

# Finite-Difference Method Without Spurious Solutions for the Hybrid-Mode Analysis of Diffused Channel Waveguides

NORBERT SCHULZ, KARLHEINZ BIERWIRTH, FRITZ ARNDT, SENIOR MEMBER, IEEE,  
AND UWE KÖSTER

**Abstract** — Diffused dielectric channel waveguides with an arbitrarily varying refractive index profile in the cross-sectional plane are analyzed with a rigorous finite-difference method formulated in terms of the wave equation for the transverse components of the magnetic field. This leads to an eigenvalue problem where the nonphysical, spurious modes do not appear. The analysis includes the complete set of hybrid modes, takes mode-conversion effects and complex waves into account, and allows the immediate inclusion of large index difference levels as well as the two-dimensional continuously varying index profile function without the usual staircase approximation. By way of example, dispersion characteristics are calculated for structures suitable for millimeter-wave and optical integrated circuits, such as channel waveguides with refractive index variations having stepped, linear, Gaussian, and exponential function profiles. The theory is verified by comparison with results available from other rigorous methods.

## I. INTRODUCTION

DIIELECTRIC channel waveguides have been the subject of growing interest for integrated circuit applications in the millimeter-wave and optical frequency range, e.g. for phase shifters, electro-optic modulators, switches, wavelength filters, and couplers [1]–[15]. As such waveguides are increasingly fabricated by ion implantation, ion exchanging, or diffusion techniques [2], [3], [5], [6], [8]–[10], [15], many structures of practical interest, such as channels with two-dimensional graded refractive index profiles, typically represented by Gaussian, complementary error, exponential, or quadratic functions, do not lend themselves to analytical solutions [11]. Therefore, in the design of integrated circuits utilizing such structures, it is important to have available a reliable computer analysis which takes the continuously varying index profile rigorously into account, is sufficiently general and flexible to allow dominant-mode and higher order mode solutions of all desired cases, and avoids the troublesome problem of nonphysical or “spurious” modes. The finite-difference formulation in this paper achieves an analysis which meets all these criteria very well.

Manuscript received April 7, 1988; revised October 30, 1989. This work was supported by the German Research Society (DFG) under Contract Ar138/7-3.

The authors are with the Microwave Department, University of Bremen, Kufsteiner Str., NW1, D-2800 Bremen 33, West Germany.

IEEE Log Number 9034885.

Methods of analyzing channel waveguides have been the subject of many papers [1]–[15]. For step index profiles, these include different kinds of mode-matching techniques [1], the finite-element analysis [3]–[5], the finite-difference method [7], [13], a modified effective-index method [12], and a Fourier transform method [14]. One-dimensional diffused channel waveguides have been analyzed by finite-element methods [3], [5], [6], by an effective index method [9], and by an iterative numerical integration method [10]. Although a number of numerical methods have already been developed for analyzing channel waveguides with a two-dimensional diffused index profile [6], [8], [15], there still exist some significant restrictions.

The single-mode investigation in [6] using a staircase approximation is based on the usual longitudinal  $E_z$ – $H_z$  finite-element formulation and, hence, contains spurious solutions. Moreover, a step approximation of graded profiles has turned out to be insufficient for many cases, especially at higher frequencies, where the field is concentrated increasingly in the smaller regions of higher permittivity. The variational finite-difference approximation in [8], based on the scalar wave equation, is valid only for small index difference levels. The quasi-TE-mode solution of [8] ignores the physical reality of hybrid modes on such waveguide structures, as well as the coupling effects [7], [18] between them. A moment method solution, such as that outlined in [15] for step basis functions applied to a circular form for the refractive index, requires changing the Green’s function for waveguides of more general inhomogeneity, and, therefore, is not considered sufficiently flexible.

In this paper, a general, flexible, versatile finite-difference formulation is presented for analyzing the hybrid-mode propagation in inhomogeneous channel waveguides (Fig. 1) with arbitrarily varying refractive index profiles  $n(x, y)$  in the cross-sectional plane and with arbitrary index difference levels. As the continuous variation of the index profile is rigorously taken into account, the method avoids the typical errors at higher frequencies inherent in a staircase approximation. A direct vector wave equation solution formulated in terms of the transverse magnetic field components  $H_x$  and  $H_y$  [7], [11], [13]

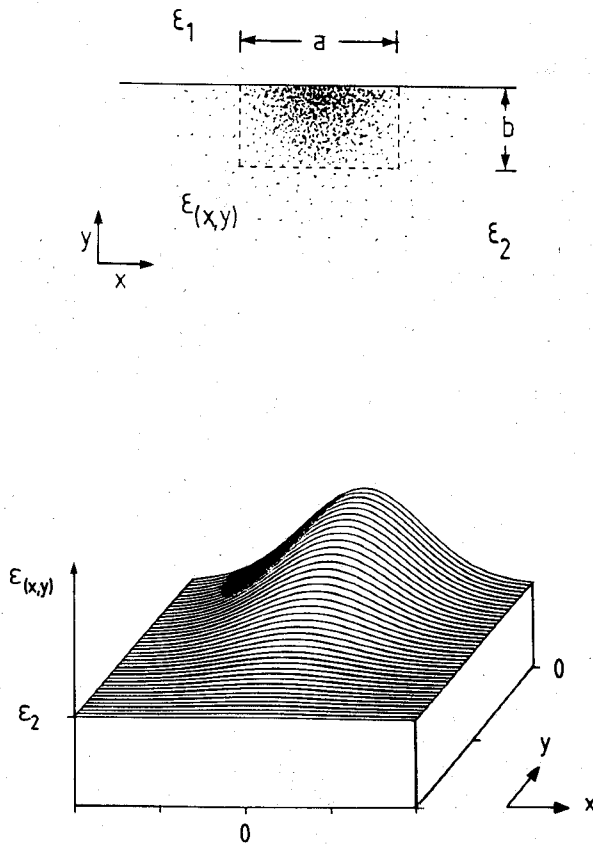


Fig. 1. Channel waveguide with arbitrarily varying index profile  $\epsilon(x, y)$  in the cross-sectional plane. Aspect ratio  $a/b$ ; plot of a Gaussian-Gaussian profile.

is utilized which leads advantageously to a standard eigenvalue problem where the zero divergence relation is implicitly included; hence, spurious modes are completely eliminated.

The analysis described takes hybrid-mode conversion effects into account, such as complex waves, at frequencies where the modes are not yet completely bound to the core of high dielectric constant, as well as at frequencies below cutoff. A graded mesh permits a numerically effective investigation of structures with realistic index profiles by making the mesh finer in regions of particular interest. Numerical results compared with available data from other rigorous methods verify the theory given.

## II. THEORY

The vector wave equation describing the wave propagation in a waveguide with inhomogeneous cross section can be expressed in terms of two field components, which are usually taken to be the longitudinal components  $E_z$  and  $H_z$  [4], [16], [23]. The formulation in terms of the transverse components  $H_x$  and  $H_y$  of the magnetic field  $\vec{H}$  is preferred, however, since it circumvents the spurious-mode problem by the implicit inclusion of the zero divergence relation [7], [13]. For the diffused channel waveguide structures to be investigated, with continuously varying permittivity  $\epsilon(x, y)$  in the cross-sectional plane (Fig. 1 illustrates a two-dimensional Gaussian profile), the

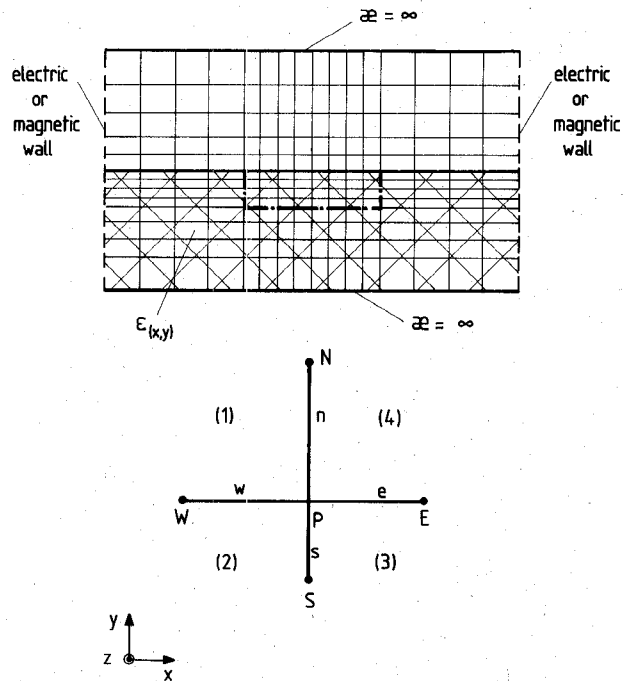


Fig. 2. Graded mesh of the five-point finite-difference representation.

finite-difference method should therefore yield a numerical solution to the vector wave equation

$$-\frac{1}{\epsilon(x, y)} \nabla^2 \vec{H} + \left[ \nabla \left( \frac{1}{\epsilon(x, y)} \right) \right] \times (\nabla \times \vec{H}) = \omega^2 \mu \vec{H} \quad (1)$$

which is derived directly from Maxwell's equations. Equation (1) may be rearranged into a set of two coupled second-order differential equations:

$$\frac{\delta^2 H_\xi}{\delta \xi^2} + \frac{\delta^2 H_\xi}{\delta \zeta^2} - \frac{1}{\epsilon} \frac{\delta \epsilon}{\delta \zeta} \frac{\delta H_\xi}{\delta \zeta} + \frac{1}{\epsilon} \frac{\delta \epsilon}{\delta \zeta} \frac{\delta H_\zeta}{\delta \xi} + [\omega^2 \mu \epsilon + \gamma_z^2] H_\xi = 0 \quad (2)$$

where  $\xi = x, y$ ,  $\zeta = y, x$ , and a  $z$  dependence of  $\exp(-\gamma_z z)$  of the wave propagation is understood. The zero divergence relation  $\nabla \cdot \vec{H} = 0$  is implicitly included in the magnetic field formulation of (1) and yields the expression for  $H_z$ :

$$H_z = \frac{1}{\gamma_z} \left[ \frac{\delta H_x}{\delta x} + \frac{\delta H_y}{\delta y} \right]. \quad (3)$$

A finite cross section is defined by enclosing the guide in a rectangular box (Fig. 2) where the sidewalls may be either electric or magnetic walls in order to include coupled structures. Although an exponential decay factor may be introduced to approximate the infinite exterior region of related "open structures" [3], in order to appropriately include mode investigations also below cutoff, it is preferred for these cases to make the box large enough [7] so that its influence on the modes may be neglected. A graded mesh, of different side lengths  $w, n, e, s$  (Fig. 2), permits the optimum use of the available computer capabilities for these cases as well.

Equations (2) are written in their five-point finite-difference form [16], which leads in this case to four coupled equations for each component  $H_\xi$  ( $\xi = x, y$ ) and which includes explicitly the function  $\epsilon(x, y)$  for the graded index profile. For the special example of an equidistant mesh, the eight resultant equations may be abbreviated in the form

$$\begin{aligned} \frac{1}{h^2} H_{\xi M_i} + \frac{1}{h^2} H_{\xi M_q} - \left( \frac{2}{h^2} \right) H_{\xi P} \pm \frac{1}{h} \frac{\delta H_\xi}{\delta \xi} \Big|_i \\ \pm \left[ \epsilon(x, y) \Big|_i \pm \frac{h}{2} \frac{\delta \epsilon(x, y)}{\delta \zeta} \Big|_i \right] \\ \cdot \frac{1}{h \epsilon(x, y)} \left| \frac{\delta H_\xi}{\delta \zeta} \right|_i + \frac{1}{2 \epsilon(x, y)} \left| \frac{\delta \epsilon(x, y)}{\delta \zeta} \frac{\delta H_\xi}{\delta \xi} \right|_i \\ + \frac{1}{2} [\omega^2 \mu \epsilon(x, y) \Big|_i + \gamma_z^2] H_{\xi P} = 0 \quad (4) \end{aligned}$$

where  $h = w = e = n = s$ ;  $M_i = W, E$ ;  $M_q = N, S$ ;  $i \in (1, 2, 3, 4)$ ;  $\xi = x, y$ ; and  $\zeta = y, x$  (cf. Fig. 2). The more general equations for graded mesh sizes used in this paper may be derived straightforwardly in the same manner.

Three sets of equivalently satisfactory boundary conditions are possible [7] to properly continue the wave solution from one subregion to the next (Fig. 2). The case chosen in this paper, which utilizes two conditions for the transversal electric and three conditions for the transversal magnetic field for each component under consideration,

$$\begin{aligned} H_x: \quad E_{z1} = E_{z2} \quad E_{z3} = E_{z4} \quad H_{z1} = H_{z2} \\ H_{z3} = H_{z4} \quad H_{z1} = H_{z4} \quad (5) \end{aligned}$$

$$\begin{aligned} H_y: \quad E_{z1} = E_{z4} \quad E_{z2} = E_{z3} \quad H_{z1} = H_{z4} \\ H_{z2} = H_{z3} \quad H_{z1} = H_{z2} \quad (6) \end{aligned}$$

has turned out to yield a slightly better convergence behavior concerning higher order modes [7].

Utilizing these conditions, the finite-difference equations (4) result in the magnetic field components at the discrete node point  $P$  in terms of the immediately adjacent node points  $W, E, N$ , and  $S$  (Fig. 2). These equations are evaluated at each node point  $P$  of the mesh, with appropriate modification to include the related boundary conditions (electric or magnetic wall) of the structure to be investigated. In this way, a set of linear homogeneous equations is derived which results in the eigenvalue equation [7]

$$[(A) - \lambda(U)](X) = 0. \quad (7)$$

Equation (7) is solved by routines of the well-known EISPACK package [17]. Complex solutions ("complex waves"), due to hybrid-mode conversion effects [7], [18], if they exist, e.g. at shielded dielectric waveguides, are included in the analysis.

The method has been verified [7] by comparisons with results available from the rigorous modal expansion

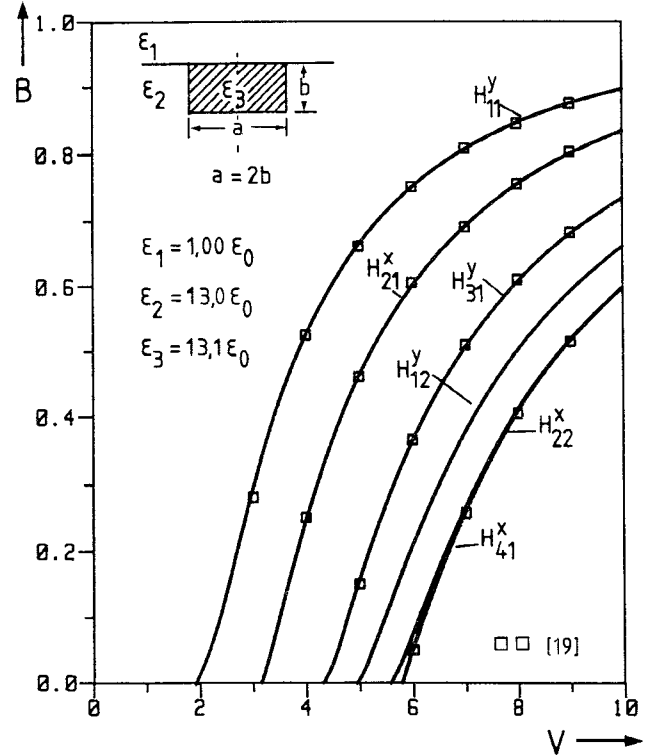


Fig. 3. Channel waveguide with a step index profile. Normalized propagation characteristic  $B$  versus normalized frequency  $V$ . Comparison with results of the mode matching method of [19].  $B = [(\beta_z/k_0)^2 - \epsilon_2]/[\epsilon_3 - \epsilon_2]$ ,  $V = k_0 \cdot b \cdot \sqrt{\epsilon_3 - \epsilon_2}$ ,  $k_0 = \omega \sqrt{\mu_0 \epsilon_0}$ .

method, e.g. for the shielded dielectric waveguide [18]. For typical structures and frequencies, for about 20 node points in the  $x$  and  $y$  directions, the error was less than about 0.05% for the first four modes. For about ten node points in each direction, the results correspond nearly to the asymptotic value; this may also be stated for higher order modes.

### III. RESULTS

For the example of an ordinary channel waveguide with step index profile, Fig. 3 compares the results of our finite-difference analysis with those of the rigorous mode-matching method in [19]. Good agreement may be stated.

Shielded dielectric waveguides (where one waveguide, the dielectric waveguide, perturbs the propagation of another one, the rectangular waveguide, and vice versa) show the effect of complex waves [18] very distinctly. Fig. 4, where the normalized propagation constants of the modes of a shielded dielectric waveguide are plotted against the permittivity, allows the modes to be assigned directly to rectangular waveguide modes ( $\epsilon_r = 1$ ) at a finite frequency (e.g. 14 GHz). Nevertheless, the plot against  $\epsilon_r$  may be considered as a (slightly distorted) dispersion curve, since increasing permittivity corresponds to a nonlinear frequency scale. Included in Fig. 4 is the evanescent mode range, whereby the corresponding real  $\alpha$  values are plotted in the same diagram but, for lucidity, in the opposite direction, as in [18]. Between  $\epsilon_r = 1 \cdots 2.4$

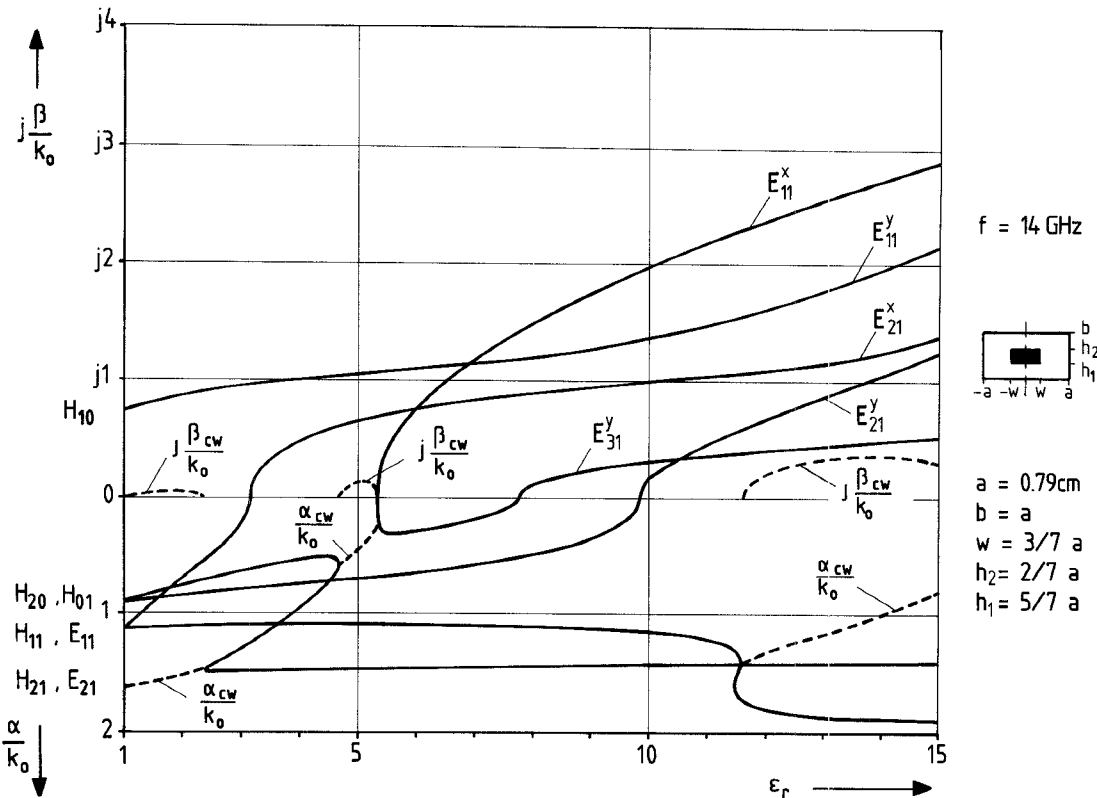


Fig. 4. Shielded dielectric waveguide. Propagation constant  $\gamma$  normalized with the free-space wavenumber plotted against permittivity  $\epsilon_r$  at  $f = 14$  GHz, calculated with the finite-difference method (--- complex waves).

and  $\epsilon_r = 4.5 \cdots 5.3$ , the eigenvalue solution leads to a complex propagation constant  $\gamma_{cw} = \pm \alpha_{cw} \pm \beta_{cw}$ , in spite of the assumption that the shielded dielectric waveguide is lossless. This effect is well known by the term *complex wave* (cf. e.g. [7] and [18]).

Since actual "open" diffused channel waveguides show no leakage effects [20], for the analysis in this paper the enclosing rectangular box is chosen to be large enough (cf. also [7]) so that its role in inducing such effects may be neglected. Furthermore, for diffused channel waveguides the propagation factors as well as the frequency are usually so normalized that there is no critical "cutoff" frequency included in the dispersion curves shown.

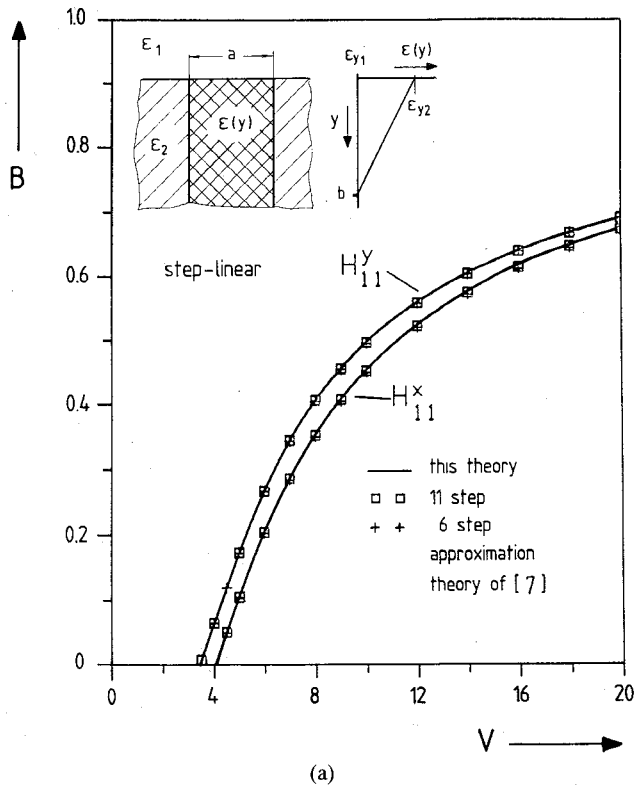
The typical CPU time required for the finite-difference analysis described may be demonstrated by the example of Fig. 4. Utilizing the magnetic wall symmetry at  $x = 0$ , and  $15 \times 15$  mesh points, the calculation of all eigenvalues involved in the matrix, and of ten related eigenvectors, requires about 4 min on a Siemens 7880 mainframe computer, while using a RAM of about 4 megabytes.

The clear advantage of the finite difference  $H_x - H_y$  formulation utilized in this paper is the complete elimination of the spurious mode problem, in contrast to the formulation in terms of the longitudinal components. This advantage, especially for the dielectric waveguiding structures under investigation, has already been illustrated in [7], where both formulations have been applied and compared at a dielectric channel guide. Moreover, the method can also include lossy structures and metallizations on planar dielectric waveguides. However, it should be men-

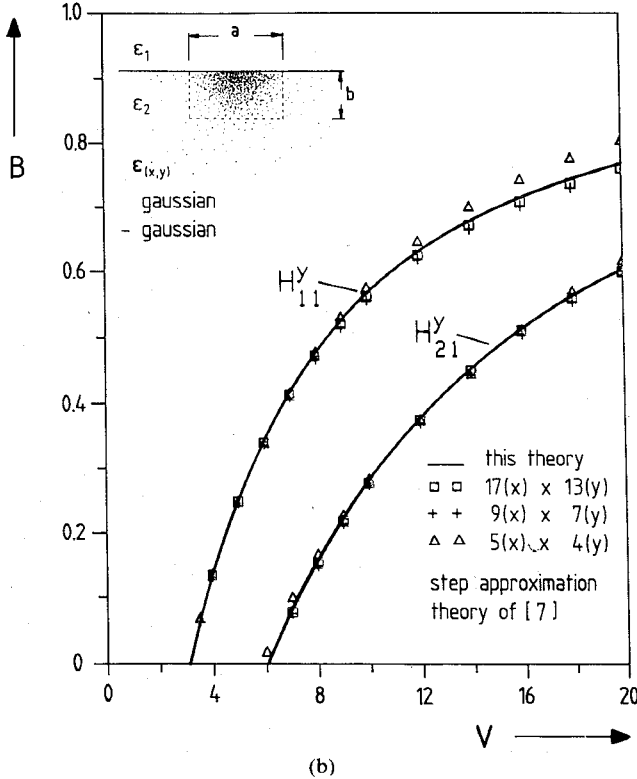
tioned that, owing to the implicit divergence relation, the  $H_x - H_y$  finite difference method would not be very appropriate for investigating the usual microwave or millimeter-wave planar or quasi-planar transmission lines (such as microstrip or finlines) with metal strips of finite thickness and very high conductivity  $\kappa \rightarrow \infty$ , as local singularities near sharp metallic edges may occur. For those structures, the conventional  $E_z - H_z$  formulation would be preferred [23].

For a channel waveguide with a step index profile in the  $x$  direction and a linear profile in the  $y$  direction, Fig. 5(a) compares the results of the rigorous finite-difference method of this paper with those of a staircase approximation by applying the finite-difference formulation for rectangular layered structures [7]. For this special one-dimensional graded structure, good agreement may be observed. However, for a more general channel waveguide with a two-dimensional graded index profile (Fig. 5(b)), the step approximation turns out to be insufficient. Assuming a Gaussian-Gaussian ( $x, y$ ) dependence of index and using the staircase approximation, good coincidence with the rigorous theory is obtained only for lower frequencies. For higher frequencies, where the field is concentrated increasingly in the smaller regions of higher permittivity, the result of the staircase approximation differs significantly from the rigorous finite difference analysis (solid line, Fig. 5(b)), especially for a small number of steps.

Fig. 6 presents the normalized propagation characteristic of a practical diffused channel waveguide with a

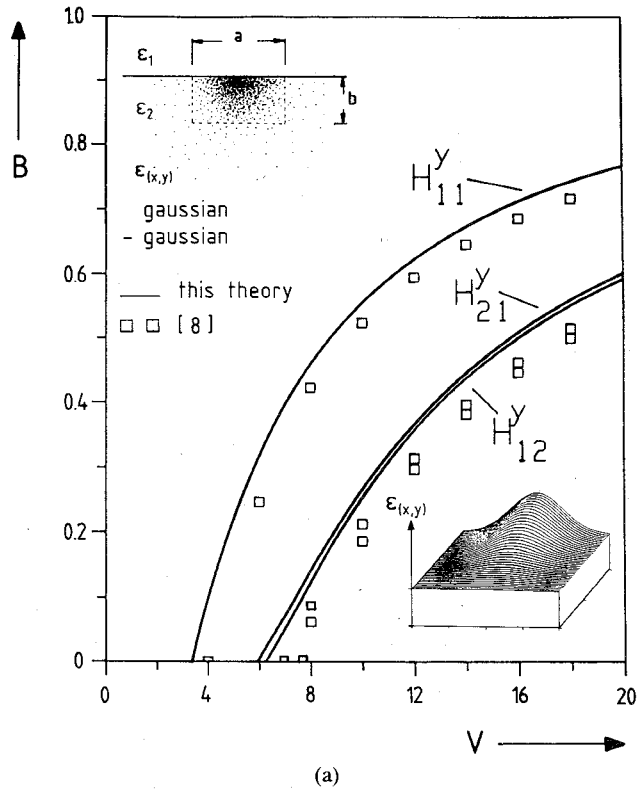


(a)



(b)

Fig. 5. Channel waveguide with continuously varying index profile. Comparison of the normalized propagation characteristic  $B$  calculated by the rigorous finite-difference formulation for continuously varying index profiles (solid lines) with that of a staircase finite-difference approximation ( $\square$ ,  $+$ ,  $\Delta$ ) [7].  $B = [(\beta_z/k_0)^2 - \epsilon_2]/[\epsilon_{\max} - \epsilon_2]$ ,  $V = k_0 \cdot a \cdot \sqrt{\epsilon_{\max} - \epsilon_2}$ ,  $k_0 = \omega \sqrt{\mu_0 \epsilon_0}$ . (a) Step index profile in  $x$  direction, linear profile in  $y$  direction:  $a/b = 1$ ,  $\epsilon_1 = \epsilon_0$ ,  $\epsilon_2 = 2\epsilon_0 = \epsilon_{y1}$ ,  $\epsilon_{y2} = 4\epsilon_0 = \epsilon_{\max}$ . (b) Two-dimensional graded index profile with a Gaussian-Gaussian ( $x, y$ ) dependence:  $a/b = 1$ ,  $\epsilon_1 = \epsilon_0$ ,  $\epsilon_2 = 2.1\epsilon_0$ ,  $\epsilon_{\max} = 1.05^2\epsilon_2$ .



(a)

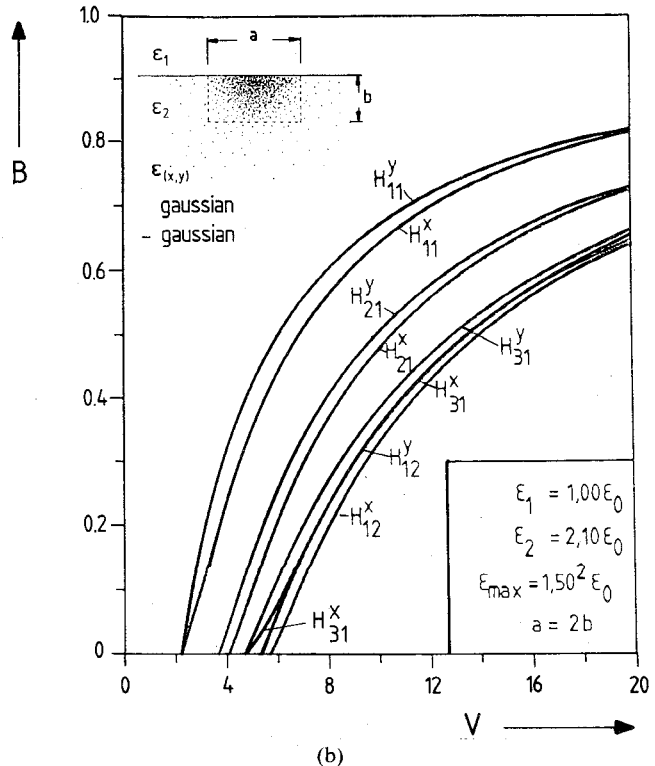
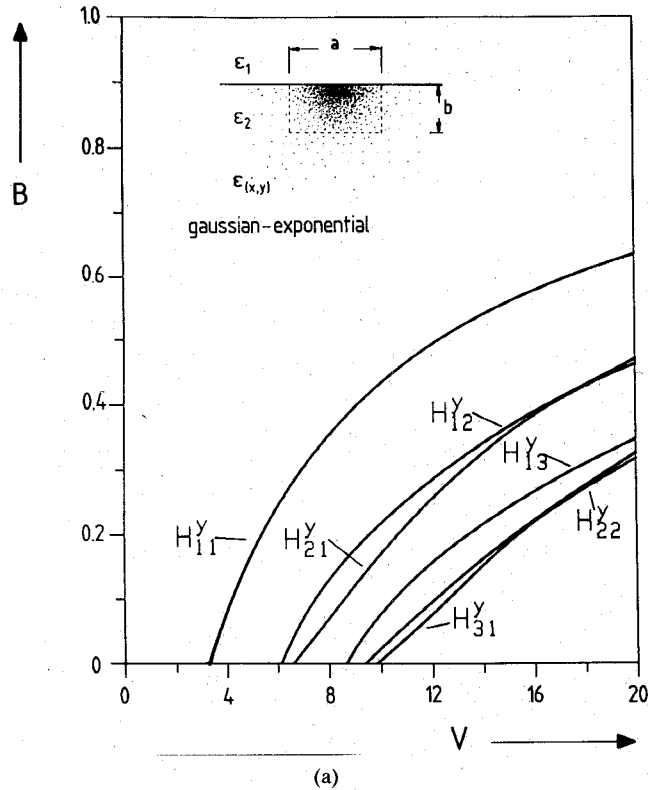
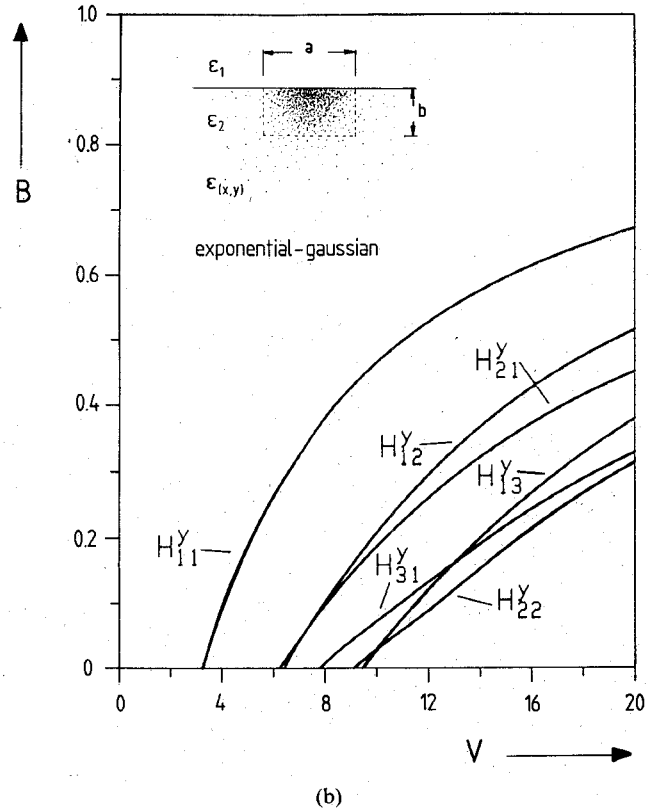


Fig. 6. Diffused channel waveguide with a Gaussian-Gaussian index profile. (a) Comparison of the normalized propagation characteristic  $B$  versus normalized frequency  $V$  with results of [8]:  $B = [(\beta_z/k_0)^2 - \epsilon_2]/[\epsilon_{\max} - \epsilon_2]$ ,  $V = k_0 \cdot a \cdot \sqrt{\epsilon_{\max} - \epsilon_2}$ ,  $k_0 = \omega \sqrt{\mu_0 \epsilon_0}$ ,  $a/b = 1$ ,  $\epsilon_1 = \epsilon_0$ ,  $\epsilon_2 = 2.1\epsilon_0$ ,  $\epsilon_{\max} = 1.05^2\epsilon_2$ . (b) Normalized propagation characteristic  $B$  versus normalized frequency  $V$  for hybrid  $H^Y$  and  $H^X$  modes.

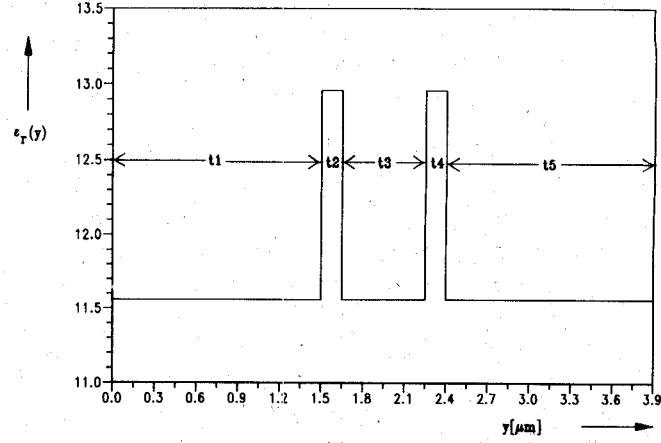


(a)

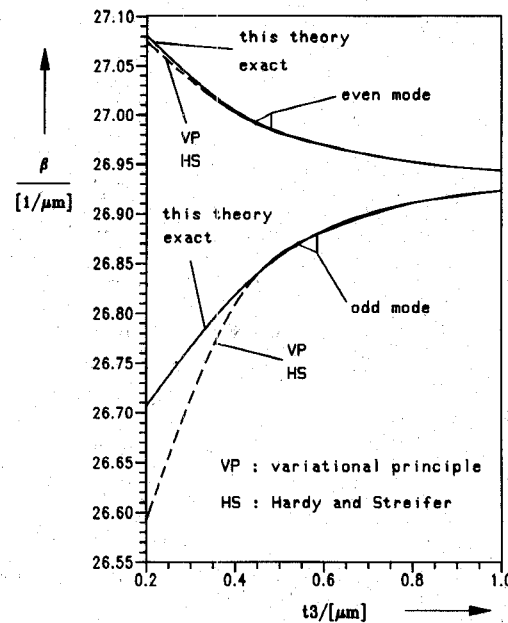


(b)

Fig. 7. Diffused channel waveguide with a Gaussian-exponential index profile. Normalized propagation characteristic  $B$  versus normalized frequency  $V$ , with  $B = [(\beta_z/k_0)^2 - \epsilon_2]/[\epsilon_{\max} - \epsilon_2]$ ,  $V = k_0 \cdot a \cdot \sqrt{\epsilon_{\max} - \epsilon_2}$ ,  $k_0 = \omega \sqrt{\mu_0 \epsilon_0}$ ,  $a/b = 1$ ,  $\epsilon_1 = \epsilon_0$ ,  $\epsilon_2 = 2\epsilon_0$ ,  $\epsilon_{\max} = 1.05^2 \epsilon_0$ . (a) Gaussian-exponential index profile. (b) Exponential-Gaussian index profile.



(a)



(b)

Fig. 8. Coupled slab waveguide structure of [21] and [22]. Comparison of the rigorous finite-difference method with the coupled mode theory. (a) Permittivity  $\epsilon_r$  versus the position  $y$  of the coupled slab waveguide. (b) Propagation constant versus waveguide spacing  $t_3$ , including the tighter coupling range, comparison with [21] and [22], and the exact results according to [22].

Gaussian-Gaussian profile [8]. Such profiles are realistic in the case of titanium diffusion in  $\text{LiNbO}_3$  and  $\text{Ag}^+ - \text{Na}^+$  ion-exchanged glass waveguides [8]. Because of the scalar wave equation TE-mode approximation in [8], only poor agreement between our exact hybrid-mode analysis and the results of [8] may be stated (Fig. 6(a)). Fig. 6(b) demonstrates the existence of additional hybrid  $H_{mn}^x$  modes on such structures, which, although in proximity, may be clearly distinguished from the  $H_{mn}^y$  propagation curves.

Since no spurious modes occur in the finite-difference analysis described, the method is appropriate for analyzing more complicated phenomena at channel waveguides with an arbitrary index distribution in the cross-sectional plane, such as hybrid-mode crossing effects (cf. Fig. 7), which have been observed at shielded rectangular dielec-

TABLE I  
COMPARISON OF THE PROPAGATION CONSTANTS OF THE SLAB WAVEGUIDE STRUCTURE (FIG. 8(a))  
ACCORDING TO [22] WITH THE RESULTS PRESENTED IN [22] (EXACT [22], VP = VARIATIONAL  
PRINCIPLE [22]; HS = COUPLED MODE THEORY OF  
HARDY AND STREIFER [21]) AND OUR THEORY

$t_3$	EXACT $\beta_1$	VP $\beta_1$	HS $\beta_1$	EXACT $\beta_2$	VP $\beta_2$	HS $\beta_2$	Our Theory	
							$\beta_1$	$\beta_2$
0.2	27.080973	27.074848	27.074770	26.706625	26.592396	26.591887	27.0809	26.7067
0.4	27.004524	27.002506	27.002435	26.818386	26.808483	26.808418	27.0045	26.8183
0.6	26.970045	26.969301	26.969296	26.883347	26.881945	26.881931	26.9700	26.8833
0.8	26.952740	26.952501	26.952501	26.911228	26.910957	26.910957	26.9526	26.9111
1.0	26.943789	26.943722	26.943722	26.923542	26.923483	26.923483	26.9437	26.9234

tric waveguides, insulated image guides, and inverted strip guides as well [1], [7], [20]. Note that such crossing effects may exist without the necessity of additional complex waves at the related frequency ranges (cf. Fig. 4). Moreover, for the class of indiffused channel waveguides shown in Fig. 7, the modes are purely bound [20]. Consequently, despite a high resolution search for complex solutions at the frequency regions where crossing effects occur, no complex waves have been observed. For a Gaussian-exponential index profile chosen by way of example, Fig. 7(a) shows that the dispersion curves of the  $H_{21}^y$  and  $H_{31}^y$  modes, which are concentrated in the region of higher permittivity with higher velocity, cross those of the  $H_{12}^y$ , and  $H_{22}^y$  modes, respectively. This effect is more pronounced for an exponential-Gaussian or parabolic-exponential index profile (not shown here).

Many results are available from the approximate coupled mode theories [21], [22]. A comparison with the rigorous finite difference method presented in this paper is considered to be particularly informative, as it might be possible to use the method reported to validate the range of applications of the coupled mode theory. Fig. 8(a) shows the example of a coupled slab waveguide structure considered in [21], [22]. The improved coupled mode theory of Hardy and Streifer shows good agreement with our results for the example reported in [22] for relatively weak coupling values ( $t_3 > 0.4 \mu\text{m}$ , cf. Fig. 8(b)). For tighter coupling, however, the results differ considerably: for the coupling region  $t_3 = 0.2 \cdots 0.4 \mu\text{m}$ , only poor agreement between our rigorous theory (which meets the exact results) and the coupled mode theory of Hardy and Streifer (HS) [21], [22], or the variational principle of [22], respectively, may be observed. A table of values (Table I) shows the differences more accurately.

#### IV. CONCLUSIONS

A rigorous finite-difference analysis for diffused dielectric channel waveguides with an arbitrarily varying refractive index profile in the cross-sectional plane is presented. The vector wave equation formulation in terms of the transverse magnetic field components circumvents the

spurious-mode problem by the implicit inclusion of the zero divergence relation. Moreover, the method takes complex waves, if they exist, into account. A graded mesh permits the optimum use of the available computer capabilities. The analysis allows the investigation of the complete set of hybrid modes on single and coupled diffused waveguide structures of practical interest, including cases of large index difference levels, and achieves the immediate inclusion of the two-dimensional continuously varying index profile function without the usual staircase approximation. Furthermore, the rigorous method described may be used to validate the range of applications of the approximate coupled mode technique. The theory given is verified by comparison with results available from other rigorous methods.

#### ACKNOWLEDGMENT

The authors wish to thank the anonymous reviewer who stimulated the comparison with the coupled mode theory presented in the paper.

#### REFERENCES

- [1] E. Goell, "A circular-harmonic computer analysis of rectangular dielectric waveguides," *Bell Syst. Tech. J.*, vol. 48, pp. 2133-2160, Sept. 1969.
- [2] H. Kogelnik, "An introduction to integrated optics," *IEEE Trans. Microwave Theory Tech.*, vol. MTT-23, pp. 2-15, June 1975.
- [3] B. M. A. Rahman and J. B. Davies, "Finite-element analysis of optical and microwave waveguide problems," *IEEE Trans. Microwave Theory Tech.*, vol. MTT-32, pp. 20-28, Jan. 1984.
- [4] B. M. A. Rahman and J. B. Davies, "Penalty function improvement of waveguide solution by finite elements," *IEEE Trans. Microwave Theory Tech.*, vol. MTT-32, pp. 922-928, Aug. 1984.
- [5] B. M. A. Rahman and J. B. Davies, "Finite-element solution of integrated optical waveguides," *J. Lightwave Technol.*, vol. LT-2, pp. 682-687, Oct. 1984.
- [6] C. Yeh, K. Ha, S. B. Dong, and W. P. Brown, "Single-mode optical waveguides," *Appl. Opt.*, vol. 18, no. 10, pp. 1490-1504, 1979.
- [7] K. Bierwirth, N. Schulz, and F. Arndt, "Finite-difference analysis of rectangular dielectric waveguide structures," *IEEE Trans. Microwave Theory Tech.*, vol. MTT-34, pp. 1104-1114, Nov. 1986.
- [8] R. K. Laga and R. V. Ramaswamy, "A variational finite-difference method for analyzing channel waveguides with arbitrary index profiles," *IEEE J. Quantum Electron.*, vol. QE-22, pp. 968-978, June 1986.
- [9] M. J. Adams, *An introduction to optical waveguides*. Chichester, England: Wiley, 1981.

- [10] J. C. Baumert and J. A. Hoenig, "Numerical method for the calculation of mode fields and propagation constants in optical waveguides," *J. Lightwave Technol.*, vol. LT-4, pp. 1626-1630, Nov. 1986.
- [11] S. M. Saad, "Review of numerical methods for the analysis of arbitrarily-shaped microwave and optical dielectric waveguides," *IEEE Trans. Microwave Theory Tech.*, vol. MTT-33, pp. 894-899, Oct. 1985.
- [12] C. M. Kim, B. G. Jung, and C. W. Lee, "Analysis of dielectric rectangular waveguide by modified effective-index-method," *Electron. Lett.*, vol. 22, pp. 296-297, Mar. 1986.
- [13] N. Schulz, K. Bierwirth, and F. Arndt, "Finite-difference analysis of integrated optical waveguides without spurious solutions," *Electron. Lett.*, vol. 22, pp. 963-965, Aug. 1986.
- [14] C. Yeh and F. Manshadi, "On weakly guiding single-mode optical waveguides," *J. Lightwave Technol.*, vol. LT-3, pp. 199-205, Feb. 1985.
- [15] Ch. Pichot, "Exact numerical solution for the diffused channel waveguides," *Opt. Commun.*, vol. 47, pp. 169-173, 1982.
- [16] J. B. Davies and C. A. Muilwyk, "Numerical solution of uniform hollow waveguides of arbitrary shape," *Proc. Inst. Elec. Eng.*, vol. 113, pp. 277-284, Feb. 1966.
- [17] B. S. Garbow, J. M. Boyle, J. J. Dongarra, and C. B. Moler, "Matrix eigensystem routines—EISPACK guide extension," in *Lecture Notes in Computer Science*, vol. 51. Heidelberg: Springer-Verlag, 1977.
- [18] J. Strube and F. Arndt, "Rigorous hybrid-mode analysis of the transition for rectangular waveguide to shielded dielectric image guide," *IEEE Trans. Microwave Theory Tech.*, vol. MTT-33, pp. 391-401, May 1985.
- [19] H. G. Unger, *Optische Nachrichtentechnik*. Heidelberg: Hüthig-Verlag, 1984.
- [20] A. A. Oliner, S.-T. Peng, T. I. Hsu, and A. Sanchez, "Guidance and leakage properties of a class of open dielectric waveguides: Part II—New physical effects," *IEEE Trans. Microwave Theory Tech.*, vol. MTT-29, pp. 855-869, Sept. 1981.
- [21] A. Hardy and W. Streifer, "Coupled mode theory of parallel waveguides," *J. Lightwave Technol.*, vol. LT-3, pp. 1135-1146, Oct. 1985.
- [22] H. A. Haus, W. P. Huong, S. Kawakami, and N. A. Whitaker, "Coupled mode theory of optical waveguides," *J. Lightwave Technol.*, vol. LT-5, pp. 16-23, Jan. 1987.
- [23] J. S. Hornsby and A. Gopinath, "Numerical analysis of a dielectric loaded waveguide with a microstrip line—Finite difference methods," *IEEE Trans. Microwave Theory Tech.*, vol. MTT-17, pp. 684-690, Sept. 1969.

**Karlheinz Bierwirth**, photograph and biography not available at the time of publication.

✉

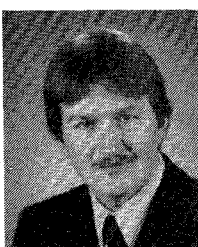
**Fritz Arndt** (SM'83) received the Dipl. Ing., Dr. Ing., and Habilitation degrees from the Technical University of Darmstadt, Germany, in 1963, 1968, and 1972, respectively.



From 1963 to 1973, he worked on directional couplers and microstrip techniques at the Technical University of Darmstadt. Since 1972, he has been a Professor and Head of the Microwave Department of the University of Bremen, Germany. His research activities center on the solution of field problems of waveguide, finline, and optical waveguide structures, antenna design, and scattering structures.

Dr. Arndt is member of the VDE and NTG (Germany). He received the NTG award in 1970, the A. F. Bulgin Award (together with three coauthors) from the Institution of Radio and Electronic Engineers in 1983, and the best paper award of the antenna conference JINA 1986 (France).

✉



**Norbert Schulz** was born in Bremethaven, Germany, on March 5, 1958. He received the Dipl. Ing. and Dr. Ing. degrees from the University of Bremen, Germany, in 1983 and 1987, respectively.

Between 1983 and 1988, he was with the Microwave Department of the University of Bremen, where he was engaged in theoretical investigations of wave propagation in dielectric waveguides. Since 1988, he has headed the Fernmeldetechnisches Amt der Stadt Bremen (Telecommunication Department of the City of Bremen).



**Uwe Köster** was born in Bremen, Germany, on October 29, 1951. He received the Dipl. Ing. degree from the University of Bremen, Germany, in 1988.

Beginning in 1988 he was with the Microwave Department of the University of Bremen, where his research dealt with numerical methods applied to integrated optical structures. Since November 1989 he has been head of a department at the Fernmeldetechnisches Amt der Stadt Bremen (Telecommunication Department

of the City of Bremen).